Steel and Composite Structures, Vol. 8, No. 6 (2008) 441-455
DOI: http://dx.doi.org/10.12989/scs.2008.8.6.441

Seismic performance assessment of steel reinforced concrete members accounting for double pivot stiffness degradation

Jia-Lin Juang and Hsieh-Lung Hsu*

Dept. of Civil Engineering, National Central University, Chung-Li, Taiwan 32054

(Received February 27, 2008, Accepted November 24, 2008)

Abstract. This paper presents an effective hysteretic model for the prediction and evaluation of steel reinforced concrete member seismic performance. This model adopts the load-deformation relationship acquired from monotonic load tests and incorporates the double-pivot behavior of composite members subjected to cyclic loads. Deterioration in member stiffness was accounted in the analytical model. The composite member performance assessment control parameters were calibrated from the test results. Comparisons between the cyclic load test results and analytical model validated the proposed method's effectiveness.

Keywords: Steel reinforced concrete; seismic performance; assessment; hysteretic model.

1. Introduction

Steel reinforced concrete (SRC) members possess sufficient stiffness and adequate ductility, and thus are effective structural designs for earthquake-resistant purposes. The seismic behavior of steel reinforced concrete members involves complicated steel-concrete interactions as well as hysteretic characteristics (El-Tawil and Deierlein 1999, Ricles and Paboojian 1994). The complicated steel-concrete interactions, such as the deterioration in the bond mechanism, the time-dependent concrete confining condition, and the various local buckling potential of the steel tube, make the seismic behavior prediction of composite members extremely difficult. To effectively evaluate the seismic performance of such members, adequate analytical models to calculate the member strength as well as the deterioration in member strength and member stiffness during the inelastic stages must be established.

In general, the hysteretic behavior of structural members can be evaluated using finite element methods (Girard and Bastien 2002, Kim *et al*. 2005, Kwan and Billington 2001, Lowes *et al*. 2004, Palermo and Vecchio 2007). However, such approaches require a large number of computations and iterations to capture the load-deformation relationships at different nodal points, and the complicated sectional and member behavior when the members are subjected to time-dependent earthquake loads. These phenomena apply to the behavior prediction of steel reinforced concrete members because performance evaluation of the composite designs raises further difficulty due to highly non-linear composite member behavior

*Corresponding Author, E-mail: t3200178@ncu.edu.tw

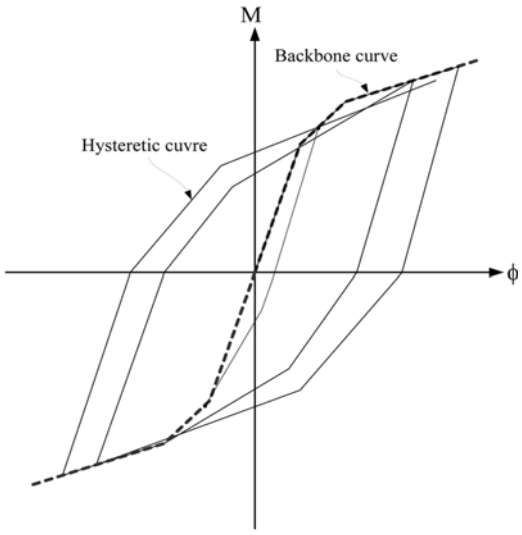

Fig. 1 Description of PHM model

which limits the practical application of the finite element method (Hsu and Liang 2003, Weng *et al*. 2001).

Alternatively, a simplified polygonal hysteretic model, as shown in Fig. 1 and denoted PHM hereafter (Sivaselvan and Reinhorn 1999), which simulates the member behavior by composing the member behavior of piece-wise linear segments can be employed. This model combines the backbone curve information obtained from the monotonic load tests and adequate strength and stiffness deterioration rules under cyclic loads to describe the member behavior in the elastic and inelastic stages. Application of piece-wise linear segment approximation is more advantageous for the evaluation of member performance under dynamic loads, because the tedious computations can be alleviated by the simplified load-deformation relationship. This model, as indicated in the investigation of Miramontes *et al*. (1996) on the frame behavior simulation, has demonstrated its effectiveness as an analytical tool in the structural analysis of steel structures and reinforced concrete designs. However, information on the composite member performance evaluation, particularly the load-deformation relationship, is still limited.

This paper focuses on the performance assessment of steel reinforced concrete members subjected to cyclic lateral loads. A series of monotonic and cyclic load tests were conducted to characterize composite member response patterns. Comparisons between the test information and the analytical results using traditional PHM model, as described in subsequent sections, demonstrated that significant discrepancies existed. Hence, an improved PHM analytical model that accounts for the member characteristics was derived. A set of control parameters for composite member performance prediction based on the test information is also proposed. Comparisons between the analytical results and test information were used to validate the effectiveness of the proposed method and establish references for design purposes.

2. Test program

In order to obtain the member responses under various loads for subsequent analyses, six steel reinforced concrete members composed of three different structural steel, ASTM A36 H200 × 100 × 5.5 × 8, H194 × 150 × 6 × 9, and H200 × 200 × 8 × 12, respectively, were fabricated for testing. All specimens possess

the same overall composite sectional dimensions, 370 mm × 370 mm, however, at different steel ratios. Longitudinal bars and the stirrups for the reinforced concrete in the composite sections were composed of #6 and #3 deformed bars, respectively. The nominal areas for #3 and #6 bars were 71.33 mm^2 and 286.52 mm^2, respectively. The compressive strength of the concrete, determined from cylinder test, was 38.5 MPa. The yield strength for structural steel was 312 MPa. The yield strengths of the #6 and #3 bars were 529.2 MPa and 563.2 MPa, respectively. Yield strains for the steel and reinforcing bars were 0.00151 and 0.00247, respectively. Spacing for the stirrups was 100 mm. Reinforcing ratio for all specimens was 0.83%. Steel ratios for the test specimens were 1.9%, 2.8%, and 4.6%, respectively. These compositions were used to investigate the behavior of typical structural members, and to evaluate the effect of structural steel on composite member performance.

Three of the specimens were used for monotonic load tests. The other specimens were used for cyclic load tests. The monotonic load tests were used to establish the backbone curves and the cyclic load tests were used to acquire the strength and stiffness deterioration rules, as required in the subsequent derivations. Specimen details and labeling are listed in Table 1. A set of servo-controlled hydraulic actuators was used to generate the required test loads. The bottom of each specimen was fastened by a pair of stiffened platforms, and rigidly attached to the strong floor, so that a fixed boundary could be achieved. The specimen top was attached to the actuator using high strength rods to transmit a lateral load. Monotonic and cyclic loads required for various tests were generated using increasing displacements and a series of prescribed increased cyclic displacement commands, respectively. The purposes of the selections were to evaluate the bearing capacities of the members and to investigate the effectiveness of the proposed model at various deformation magnitudes. The displacement histories used for testing are shown in Fig. 2 Structural responses of the composite members were measured using the installed strain gages, linear variable displacement transducer (LVDT), and the tiltmeters. The specimen details, measurement arrangements and the test set-ups are shown in Fig. 3 Experimental information was gathered by data acquisition system for later analyses.

3. Failure patterns and member responses

For members subjected to lateral load, similar flexural cracks were first observed at the member bottoms where maximum bending moments were exhibited. The cracks expanded when the magnitudes

Table 1. Specimen details

Test group	Specimen	Dimension B x D(mm)	Steel section d_s x b_f x t_w x t_f(mm)	Longitudinal bars	$\frac{(EI)_S}{(EI)_{SRC}}$
Monotonic load test	SRC100 m	370 × 370	H200 × 100 × 5.5 × 8	4-#6	0.225
	SRC150 m	370 × 370	H194 × 150 × 6 × 9	4-#6	0.299
	SRC200 m	370 × 370	H200 × 200 × 8 × 12	4-#6	0.437
Cyclic load test	SRC100c	370 × 370	H200 × 100 × 5.5 × 8	4-#6	0.225
	SRC150c	370 × 370	H194 × 150 × 6 × 9	4-#6	0.299
	SRC200c	370 × 370	H200 × 200 × 8 × 12	4-#6	0.437

Note:
B = width of composite section; D = depth of composite section, d_s = depth of steel section,
b_f = flange width of steel section, t_w = web thickness of steel section, t_f = flange thickness of steel section,
$(EI)_S$ = equivalent flexural rigidity of the structural steel, $(EI)_{SRC}$ = equivalent flexural rigidity of the composite section

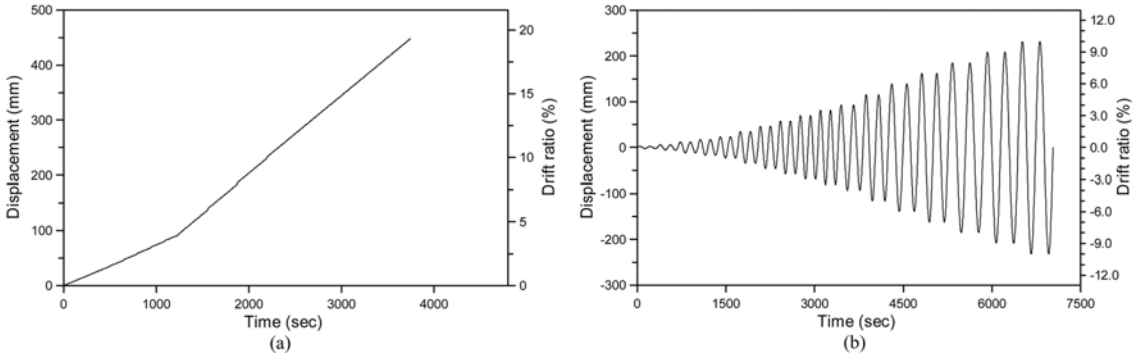

Fig. 2 Displacement histories: (a) monotonic load test; (b) cyclic load test

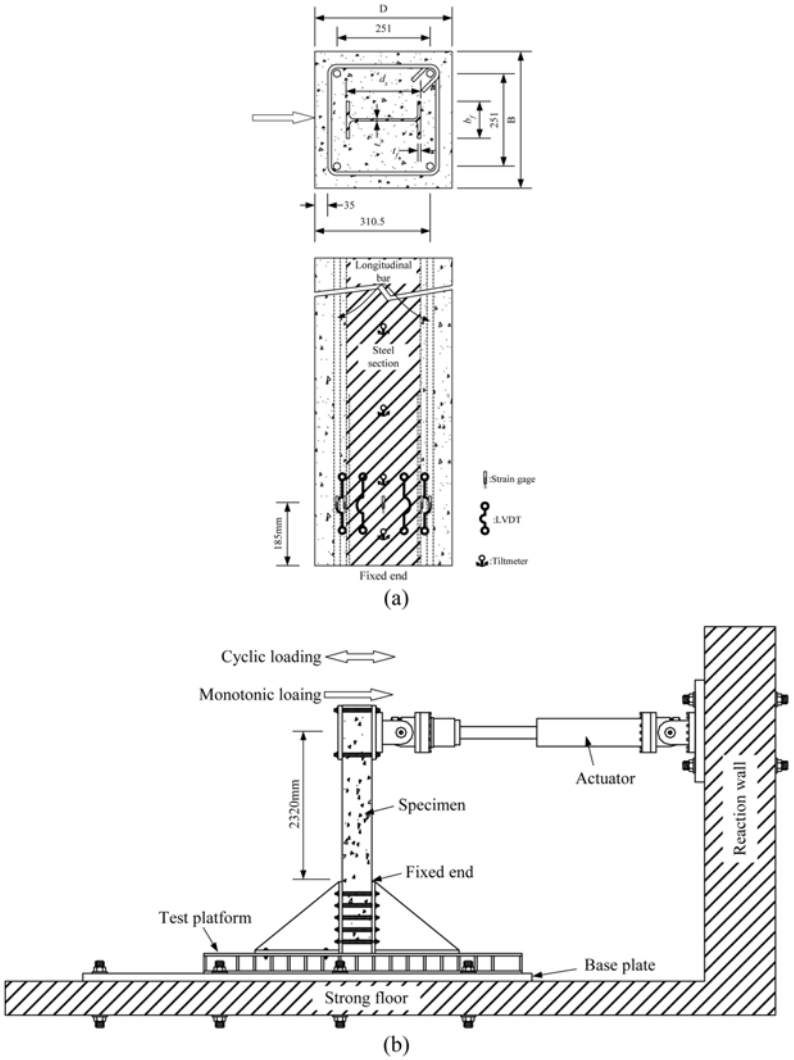

Fig. 3 Experimental details: (a) cross-section and measurement arrangements for specimen; (b) test set-ups

of the applied lateral displacements increased. Buckling of the longitudinal bars was observed when the member reached the maximum strength. In the monotonic loading tests, concrete crushing due to vertical cracks at the compression side of the member bottoms was observed. However, alternation of compression and tension at the member bottoms was introduced when cyclic lateral load was applied. This mechanism led to the formation of plastic hinge at the member's confined region.

Fig. 4 shows the typical failure patterns, SRC150 m and SRC150c at 9% drift, for members subjected to monotonic and cyclic loads. The figure shows that the damaged areas of the members were limited to the section perimeters. The sectional core integrity was effectively sustained because of the adequate steel-concrete composite mechanism. This mechanism prevented possible local steel buckling at large deformation and allowed effective member strength development in the strain-hardening stages. These phenomena explained the significant performance of composite members when subjected to seismic loads.

Fig. 5 shows the load-deformation relationships for the tested members. The yielding displacement, the ultimate displacement, defined by the displacement when member strength dropped to 90% of the maximum strength; and the corresponding ductility for the test specimens are listed in Table 2. It can be observed from the comparison that the achievable yielding displacement is higher for member with larger steel ratio. It can also be found from the figure that the strength envelope of member subjected to cyclic load follows the backbone curve of member subjected to monotonic load alone, except that the achievable deformation in the former case is smaller. This figure validates that the strength reduction was minor even when the specimen was subjected to large deformation. Therefore, the effect of strength deterioration in affecting the performance assessment of steel reinforced concrete members can be reasonably neglected. However, for members subjected to cyclic loads, the member stiffness at various deformations was significantly influenced, as shown in the figure. This phenomenon incurred significant performance deteriorations, including changes in corresponding deformation and energy dissipation, and therefore must be adequately investigated so that effective performance assessment could be accomplished. Relationships between the member performance assessment and the stiffness degradation were correlated and defined in the following sections.

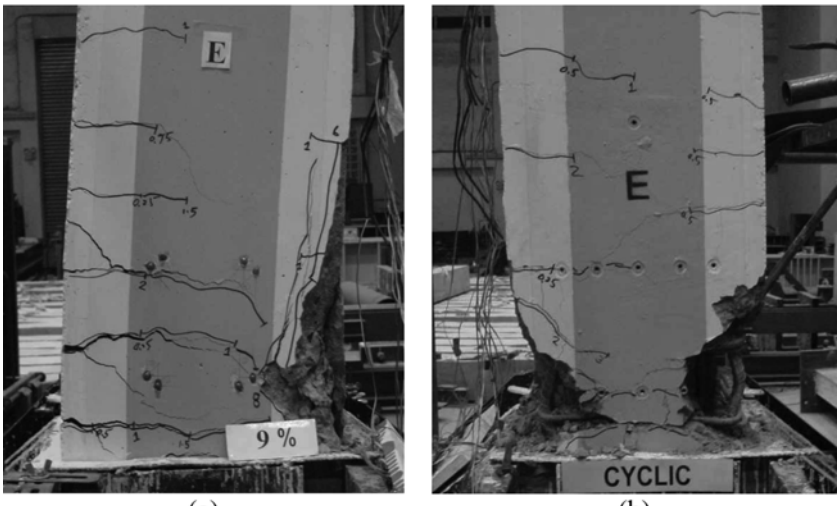

(a) (b)

Fig. 4 Typical failure patterns of members: (a) monotonic load test; (b) cyclic load test

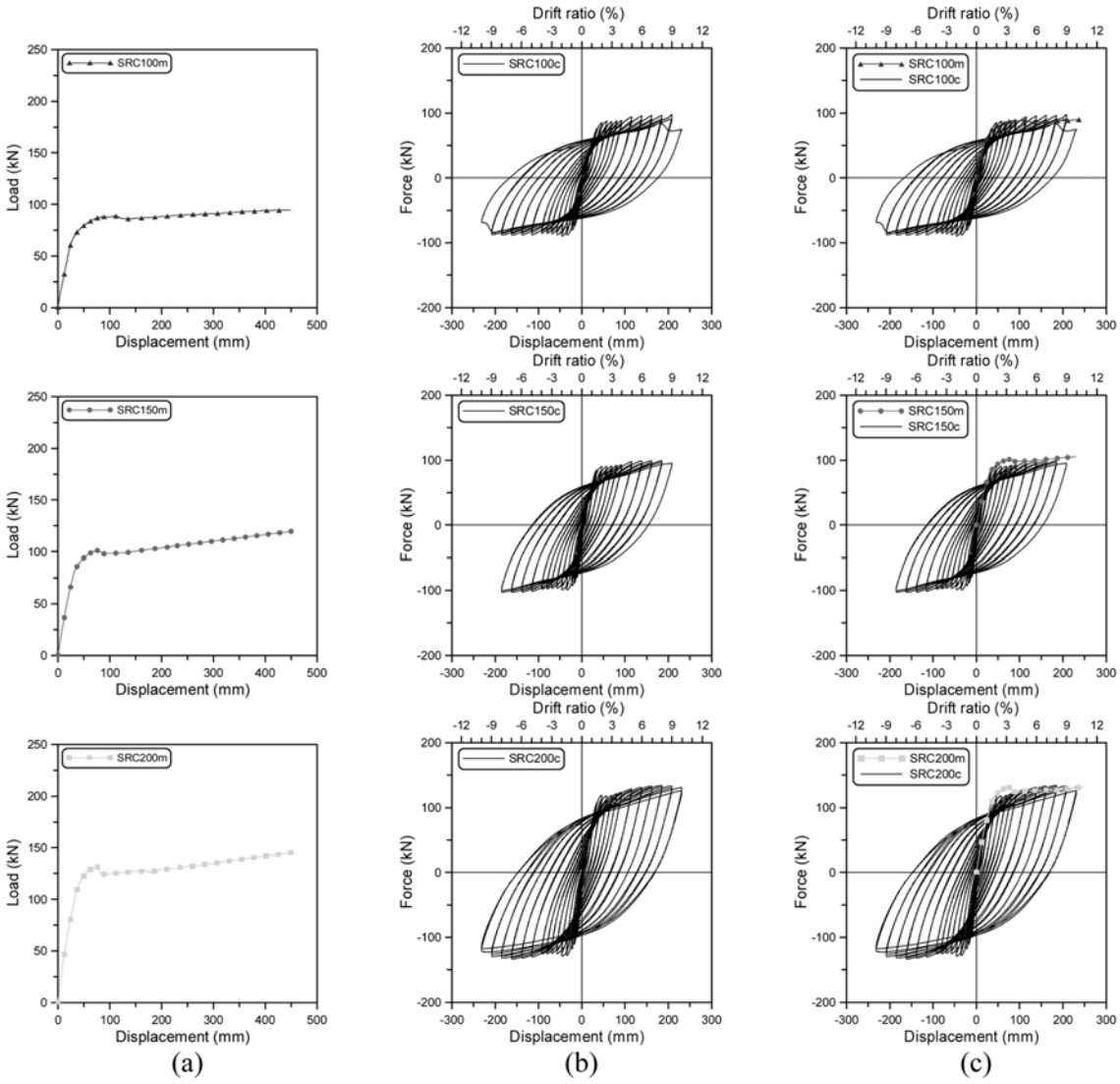

Fig. 5 Load-deformation relationships: (a) monotonic load tests; (b) cyclic load test (c) comparisons

4. Stiffness deterioration

It has been indicated in several research studies that the stiffness deterioration of members is greatly influenced by the deformation patterns during the load excitation. For example, the stiffness deterioration of a member subjected to repeated loads is more significant than that of a member subjected to a monotonic load alone. Therefore, adequate evaluation of member stiffness subjected to cyclic loads is essential to the effective performance assessment of members subjected to earthquake loads. According to several cyclic loading test results (Kunnath *et al*. 1990, Takeda *et al*. 1970), the unloading stiffness of reinforced concrete members at various deformation stages coincided at a pivot point, as shown in Fig. 6. Analytical method adopting this phenomenon, referred as the pivot model, were often used to

Table 2 Responses of the test specimens

Specimen	Steel ratio (%)	Reinforcing ratio (%)	Yielding displacement (mm)	Ultimate displacement (mm)	Yielding strength (kN)	Max strength (kN)	Ductility
SRC100 m	1.9	0.83	31.2	460.4*	69.1	96.8	14.7*
SRC150 m	2.8	0.83	32.4	460.4*	81.7	108.2	14.2*
SRC200 m	4.6	0.83	39.6	460.4*	113.2	148.5	11.6*
SRC100c	1.9	0.83	31.4	208.2	70.3	93.85	6.6
SRC150c	2.8	0.83	33.5	209.9	84.1	99.3	6.2
SRC200c	4.6	0.83	39.4	231.2	113.9	134.3	5.9

Note: *Values were measured when tests were stopped due to excessive displacements.

describe the inelastic behavior of such members at large deformation. According to the pivot model, the deteriorated member stiffness at inelastic stages, K_r, is determined by multiplying the elastic stiffness, K_0, by a reduction factor, R_K, as follows:

$$K_r = R_K K_0 \tag{1}$$

In the above expression, the reduction factor is affected by the magnitude of the deformation and the corresponding strength during the load history. They can be related by the following expression (Park *et al*. 1987):

$$R_K = \frac{M_m + \alpha M_y}{K_0 \phi_m + \alpha M_y} \tag{2}$$

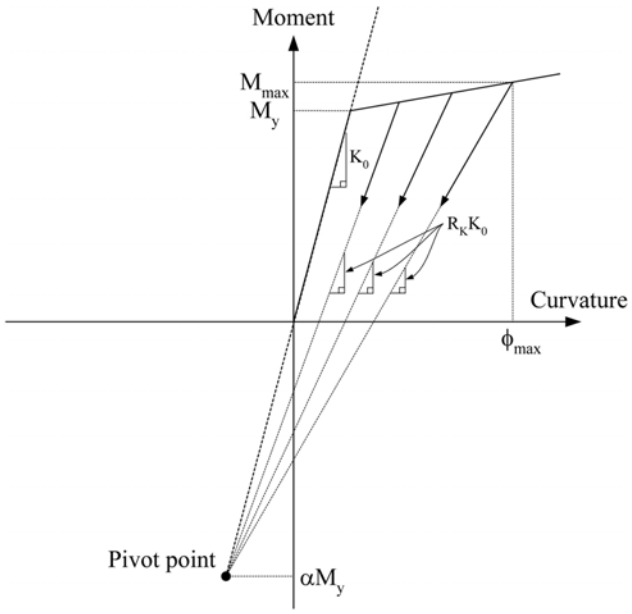

Fig. 6 Description of typical pivot behavior in reinforced concrete members

in which ϕ_m is the largest curvature under cyclic loading, α is a positive number that determines the pivot point location, M_y is the yielding moment, and M_m is the moment with respect to ϕ_m. The α value used in Eq. (2) can be evaluated by the ratio between the moment corresponding to the pivot point on the member's unloading curves and the yielding moment. This value varies with the sectional geometry and can be determined using test information. The pivot model usually provides sufficient accuracy when used to describe the behavior of reinforced concrete members (Sivaselvan and Reinhorn 1999).

Although steel reinforced concrete member designs also involve the characteristics of the reinforced concrete, significant discrepancy was raised when the pivot model was used to predict the hysteretic behavior of the composite members. Fig. 7 compares the member stiffness obtained from tests and the analytical results using the above-mentioned pivot model. In this figure, the member's normalized stiffness, defined by the ratios between the member stiffness at various deformations and the elastic stiffness, and the curvature ductility, evaluated by the ratios between the curvature at the corresponding deformations and the yielding curvature, was correlated. It can be found from the comparisons that these two values agreed with each other when members were subjected to smaller deformations. However, significant discrepancies were observed when the members reached larger deformations. It was obtained from the test results that the curvature ductilities at which members exhibited two pivot point behavior were 5.32, 4.35, and 3.52 for the tested members: SRC100c, SRC150c, and SRC200c, respectively. The difference between the measured stiffness and the analytical results was divided by the measured one to evaluate the magnitude of error. The relationship between the discrepancy in measured stiffness and the corresponding member deformation, as shown in Fig. 8, further validated the importance and necessity of defining an effective stiffness deterioration model for member performance assessment.

5. Proposed double pivot model

Fig. 9 shows the moment-curvature relationships for members subjected to cyclic loads. It can be found from the figure that the unloading stiffness of the member at various deformations was different because the sectional integrity deteriorated due to progressive concrete crushing. Therefore, the member's unloading stiffness was determined by the lines that connected the unloading points and the points at

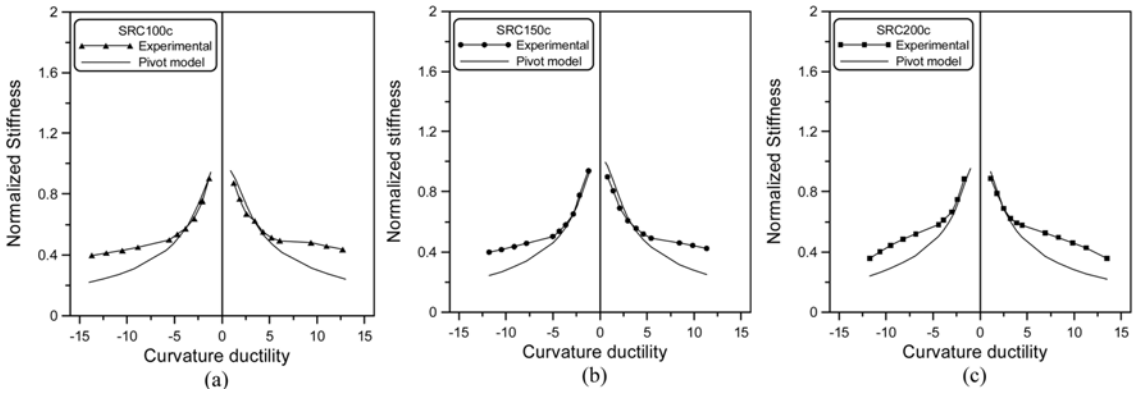

Fig. 7 Comparisons of normalized stiffness between experimental results and values from pivot model: (a) SRC100c; (b) SRC150c; (c) SRC200c

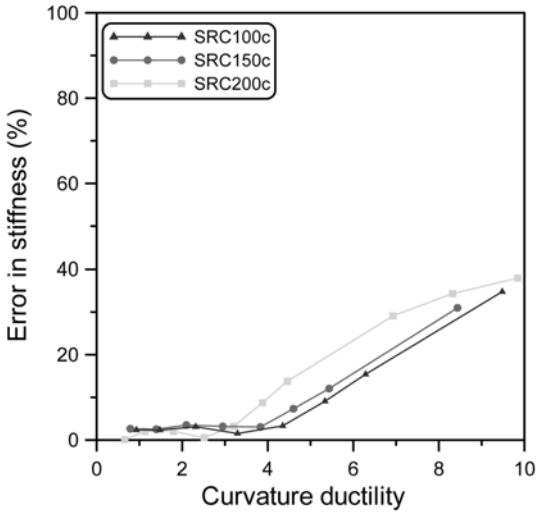

Fig. 8 Error in stiffness between the experimental result and the values from pivot model

zero load. In this figure, double pivot points, instead of a single point as indicated in the previous pivot model, were exhibited when the members were subjected to cyclic loading. These two points connected the unloading curves when members were subjected to smaller and larger deformations, respectively. The curvature that distinguished these two groups was approximately 0.045. This phenomenon indicated that a modification in the analytical procedures, denoted as the proposed double pivot model hereafter, was necessary, in order to achieve adequate seismic performance assessment of steel reinforced concrete members.

As shown in Fig.10, the location of the first pivot point, defined by the intersecting position of the unloading curves when a member is subjected to smaller deformations, can be determined using the following values:

$$\phi_{pv1} = -\frac{\alpha M_y}{K_0} \tag{3}$$

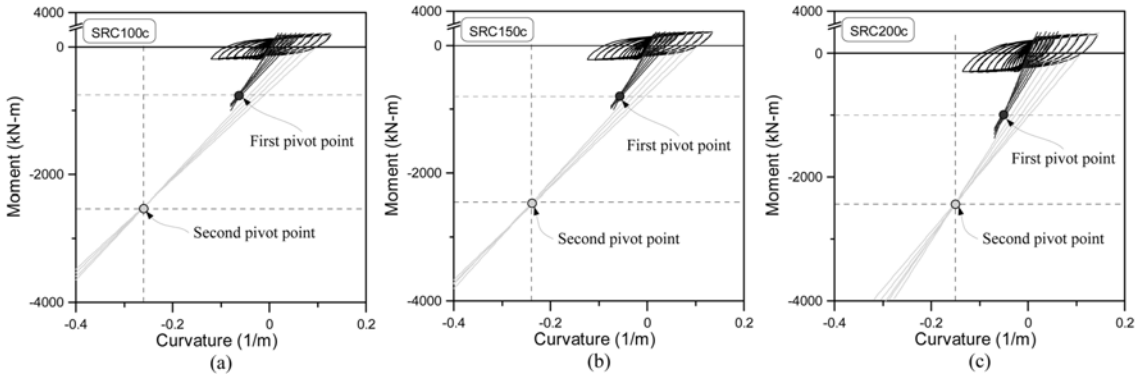

Fig. 9 Hysteretic behavior of SRC members with double pivot points; (a) SRC100c; (b) SRC150c; (c) SRC200c

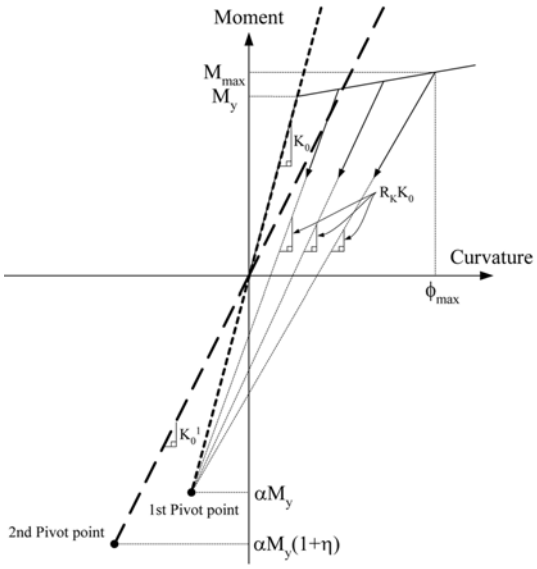

Fig. 10 Relationship among moment, curvature and double pivot points

$$M_{pv1} = -\alpha M_y \tag{4}$$

in which ϕ_{pv1} and M_{pv1} are the curvature and the moment, respectively, corresponding to the first pivot point, and α is a coefficient determined using the test information. Therefore, the stiffness reduction factor at this stage, R_{K1}, can be expressed as:

$$R_{K1} = \frac{M_{\max} + \alpha M_y}{K_0 \phi_{\max} + \alpha M_y} \tag{5}$$

in which $M_{\max}$ and $\phi_{\max}$ are the achieved maximum moment and the corresponding curvature during the load history.

Shifting the first pivot point to a lower position, defined as the second pivot point, was observed when the member deformation was increased. Also shown in Fig. 10, this point can be determined using the following expressions:

$$\phi_{pv2} = \frac{\alpha M_y (1 + \eta)}{K_0^1} \tag{6}$$

$$M_{pv2} = -\alpha M_y (1 + \eta) \tag{7}$$

in which ϕ_{pv2} and M_{pv2} are the curvature and the moment, respectively, corresponding to the second pivot point, η is an experimentally-determined coefficient accounting for the shift in pivot points, and K_0^1 is the stiffness when the member first reached the softening stage. Major difference between the original pivot model and the proposed double pivot model is the shifting of pivot points observed in the

latter case. This phenomenon reflects the particular softening behavior of steel-concrete composite members at large deformation, and must be noted when adequate structural response simulation is desired.

To account for the softening characteristics of the member at large deformation, a further reduction factor η_K was defined:

$$\eta_K = \frac{K_0^1}{K_0} \tag{8}$$

Therefore, the stiffness reduction factor at second pivoting stage, denoted R_{K2}, can be evaluated using the following expression:

$$R_{K2} = \frac{M_{\max} + \alpha M_y(1+\eta)}{\eta_K K_0 \phi_{\max} + \alpha M_y(1+\eta)} \tag{9}$$

The relationships between the stiffness reduction parameters and the compositions of the tested members are shown in Fig. 11. This figure shows that these parameters can be correlated with the flexural rigidity ratio between the structural steel and the composite section using linear approximation, and can be expressed as follows:

$$\alpha = -5.144\frac{(\mathrm{EI})_\mathrm{S}}{(\mathrm{EI})_\mathrm{SRC}} + 5.774 \quad \text{for} \quad 0.2 \le \frac{(\mathrm{EI})_\mathrm{S}}{(\mathrm{EI})_\mathrm{SRC}} \le 0.45 \tag{10}$$

$$\eta_K = 0.821\frac{(\mathrm{EI})_\mathrm{S}}{(\mathrm{EI})_\mathrm{SRC}} + 0.368 \quad \text{for} \quad 0.2 \le \frac{(\mathrm{EI})_\mathrm{S}}{(\mathrm{EI})_\mathrm{SRC}} \le 0.45 \tag{11}$$

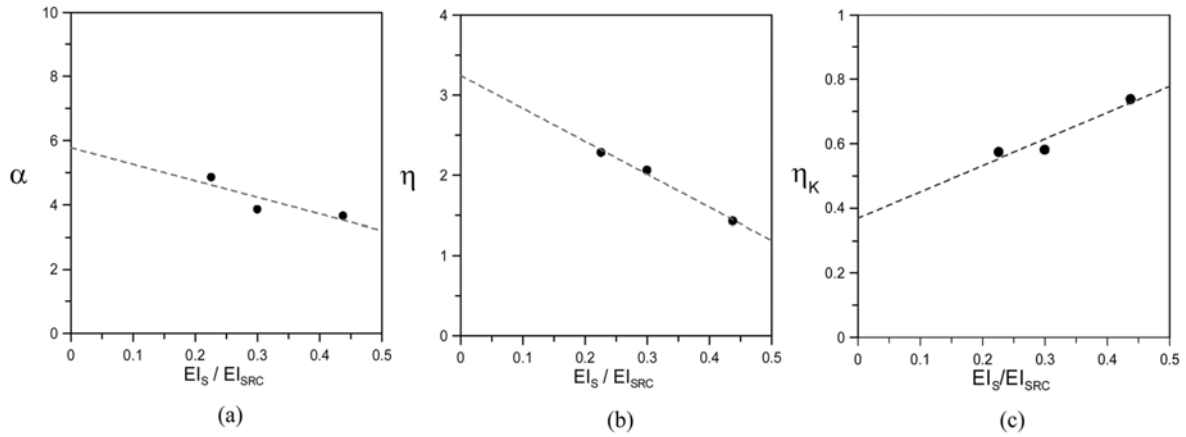

Fig. 11 Relationship between stiffness reduction parameters and flexural rigidity ratios of composite sections: (a) α values; (b) η values; (c) η_K values

$$\eta = -4.108\frac{(EI)_S}{(EI)_{SRC}} + 3.243 \quad \text{for} \quad 0.2 \le \frac{(EI)_S}{(EI)_{SRC}} \le 0.45 \tag{12}$$

in which $(EI)_S$ and $(EI)_{SRC}$ are the equivalent flexural rigidities of the structural steel and the composite section, respectively. Average errors between the experimental and analytical results for α, η_K, and η of the tested specimens were 6%, 3.5%, and 1.7%, respectively. These values showed close relevance and validated the effectiveness of the proposed expressions. Therefore, the information can be used to describe the member's hysteretic behavior, define the member performance for engineering practices, and be further refined with more experimental information.

6. Validation of the proposed method

To validate the adequateness of the proposed parameters for the proposed double pivot model to predict the behavior of the composite members, the experimental and analytical load-deformation relationships for the test specimens were compared. Fig. 12 describes the analytical processes to determine the member's hysteretic relationship. During the analytical processes, the maximum deformation experienced in the loading history, referred to as the vertex value, was used to evaluate the required reduction factors for subsequent analyses. The hysteretic curves of the test specimens are compared with those obtained from the proposed processes, as shown in Fig. 13. Effectiveness of the proposed method can be first justified by the differences in residual displacements between the analytical and experimental results. For example, the maximum residual displacement discrepancy for the test specimens was less than 1.6% when members reached 7% drift. The accuracy in deformation estimation validated the effectiveness of the proposed model.

Comparisons of member unloading stiffness between the experimental results and the analytical results obtained from the proposed double pivot model are shown in Fig. 14. It can be obtained from the results that the maximum discrepancy in initial unloading stiffness is less than 2.8%, obtained in SRC100c specimen. It can also be found from the comparisons that significant improvements in stiffness predictions was achieved. The effectiveness of the proposed model was further evaluated using the energy dissipation, defined by the area bounded by the hysteretic loops, of the tested members. Comparisons of the cumulative energy dissipation between the analytical and test results, as shown in Fig. 15, justified the applicability of the proposed method.

In order to further investigate the effectiveness of the proposed method, the double pivot model was adopted to evaluate the structural responses of a composite member selected from the literature (Hsu *et al.* 2004). Composite section used in this example was composed of JIS SS400-grade H150 × 100 × 6 × 9 steel and reinforced concrete. Yield strengths of the steel (f_{ys}) and the reinforcing bars (f_{yb}) were 325 MPa and 394 MPa, respectively. Compressive strength of the concrete was 27.9 MPa. Sectional details are shown in Fig. 16. The load-deformation relationships obtained from the test and from using the proposed double pivot model are also compared in Fig. 16. It can be found from the comparisons that the discrepancy in cumulative energy is small, less than 2.1%, and the maximum discrepancy in residual displacement is also minor, approximately 4%. The significant relevance validated the effectiveness of the proposed method.

7. Conclusions

This paper presented test information on steel reinforced concrete members subjected to monotonic

Fig. 12 Analytical process for hysteretic relationship determination

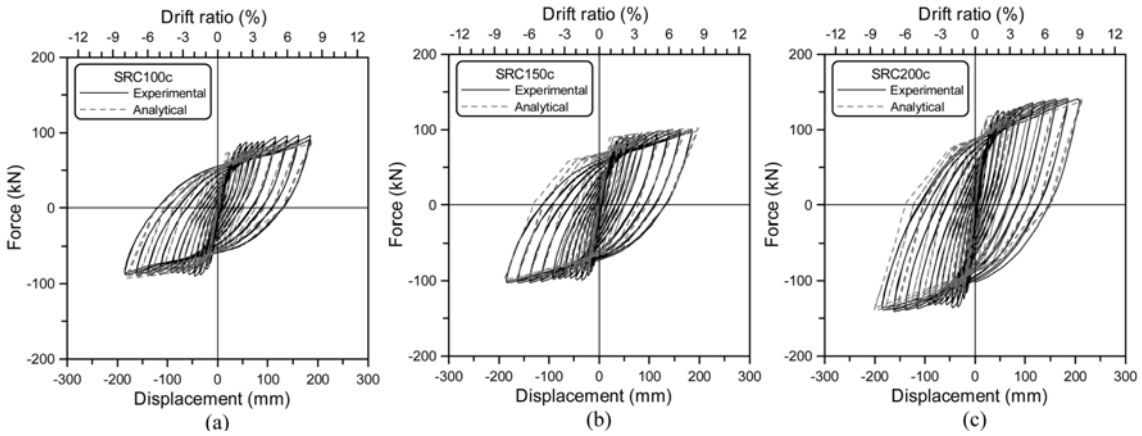

Fig. 13 Comparisons of hysteretic behavior between experimental results and values from proposed double-pivot model: (a) SRC100c; (b) SRC150c; (c) SRC200c

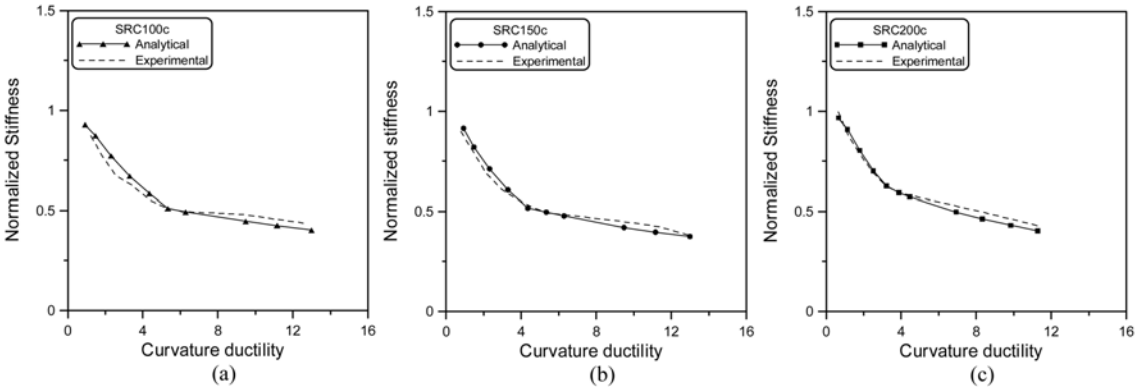

Fig. 14 Comparisons of member stiffness between experimental results and values from proposed double-pivot model: (a) SRC100c; (b) SRC150c; (c) SRC200c

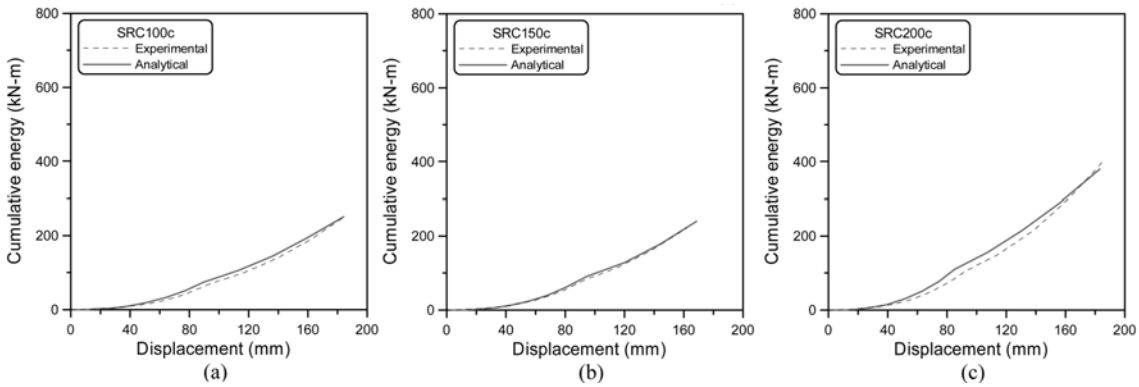

Fig. 15 Comparisons of member energy dissipations:(a) SRC100c; (b) SRC150c; (c) SRC200c

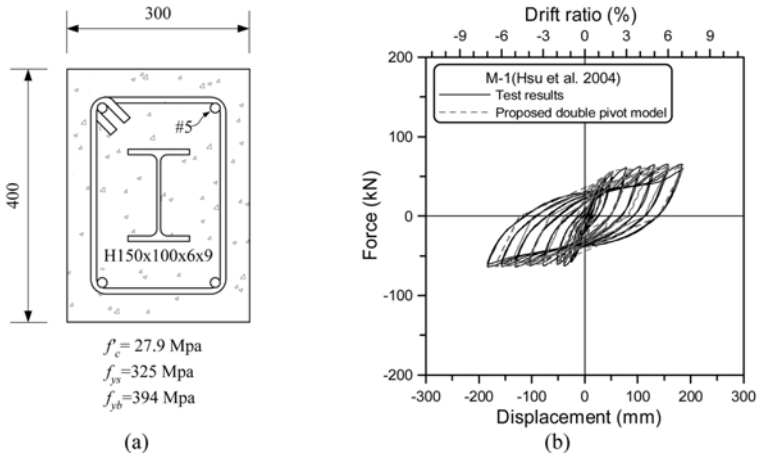

Fig. 16 Validation of proposed double pivot model: (a) specimen from literature for comparison; (b) load-deformation relationship

and cyclic loads. An effective hysteretic model, accounting for the double pivot point characteristics of composite members, for the prediction and evaluation of member performance subjected to cyclic loading was proposed. It was found from the tests that the achievable yield and ultimate displacements were larger for members with higher steel ratios. It was also found from the test results that the curvature that distinguished the two pivot points was approximately 0.045. A set of structural parameters for double pivot model simulation of member responses, such as α, η_K, and η were calibrated from the test results. Significant relevance in energy dissipation and residual displacement between the test information and the analytical results validated the effectiveness of the proposed method.

Acknowledgements

This study was partially supported by the National Science Council of the Republic of China under Grant No. NSC 93-2221-E-008-021, which is gratefully acknowledged.

References

El-Tawil, S. and Deierlein, G.G. (1999), "Strength and ductility of concrete encased composite columns", *J. Constr. Steel Res*., **55**(9), 1009-1019.

Girard, C. and Bastien, J. (2002), "Finite-element bond-slip model for concrete columns under cyclic loads", *J. Struct. Eng.-ASCE*, **128**(12), 1502-1510.

Hsu, H.L. and Liang, L. L. (2003), "Performance of hollow composite members subjected to cyclic eccentric loading", *Earthq. Eng. Struct. Dyn*., **32**(3), 443-461.

Hsu, H.L., Hsieh, J.C. and Juang, J.L. (2004) "Seismic performance of steel-encased composite members with strengthening cross inclined bars", *J. Constr. Steel Res*., **60**(11), 1663-1679

Kim, T.H., Lee, K.M., Chung, Y.S., and Shin, H.M. (2005), "Seismic damage assessment of reinforced concrete bridge columns", *Eng. Struct*., **27**(4), 576-592.

Kunnath, S. K., Reinhorn, A. M. and Park, Y. J. (1990), "Analytical modeling of inelastic seismic response of R/C structures", *J. Struct. Eng.-ASCE*, **116**(4), 996-1017.

Kwan, W.P. and Billington. S.L. (2001), "Simulation of structural concrete under cyclic load", *J. Struct. Eng.-ASCE*, **127**(12), 1391-1401.

Lowes, L.N., Moehle, J.R. and Govindjee, S. (2004) "Concrete-steel bond model for use in finite element modeling of reinforced concrete structures", *ACI Struct. J*., **101**(4), 501-11.

Miramontes, D., Merabet, O. and Reynouard, J. M. (1996), "Beam global-model for the seismic analysis of RC frames", *Earthq. Eng. Struct. D.*, **25**(7), 671-688.

Palermo, D. and Vecchio, F.J. (2007), "Simulation of cyclically loaded concrete structures based on the finite-element method", *J. Struct. Eng.-ASCE*, **133**(5), 728-738.

Park, Y. J., Reinhorn, A. M. and Kunnath, S. K. (1987), IDARC: Inelastic damage analysis of reinforced concrete frame - shear-wall structures, NCEER-87-0008. State University of New York at Buffalo, NY.

Ricles, J.M. and Paboojian, S.D. (1994), "Seismic performance of steel-encased composite columns", *J. Struct. Eng.-ASCE*, 120(8), 2474-2494.

Sivaselvan, M. V. and Reinhorn, A. M. (1999), Hysteretic models for cyclic behavior of deteriorating inelastic structures, MCEER-99-0018. State University of New York at Buffalo, NY.

Takeda, T. A., Sozen, M. A. and Nielsen, N. N. (1970), "Reinforced concrete response to simulated earthquake", *J. Struct. Div.-ASCE*, **96**(ST-12), 2557-2573.

Weng, C. C., Yen, S. I. and Chen, C. C. (2001), "Shear-strength of concrete-encased composite structural members", *J. Struct. Eng.-ASCE*, **127**(10),1190-1197.

CC